Pinning Forces and Lower Critical Fields in $YBa_2Cu_3O_y$ Crystals: Temperature Dependence and Anisotropy

Dong-Ho Wu and S. Sridhar
Department of Physics, Northeastern University, Boston, Massachusetts 02115
(Received 20 July 1990)

Measurements of the field-dependent radio-frequency penetration depth $\lambda(H,T)$ are used to delineate the lower-critical-field H_{c1}-T phase boundary, and to study flux dynamics, in $YBa_2Cu_3O_y$ crystals. For both $\mathbf{H}\parallel\hat{\mathbf{c}}$ and $\mathbf{H}\perp\hat{\mathbf{c}}$, H_{c1} obeys a BCS temperature dependence, with a temperature-independent anisotropy of 3.4 ± 0.3. In the mixed state, the data obey $\lambda^2(H)=[\phi_0/\mu_0\alpha(T)]B(H)$, and yield both the functional dependence $B(H)$ and the pinning force constant $\alpha(T)$. The latter is anisotropic, obeys an approximately $(1-t^2)^2$ temperature dependence, and vanishes slightly below the bulk transition temperature.

PACS numbers: 74.30.Ci, 74.60.Ec, 74.60.Ge, 74.70.Vy

The high-T_c superconductors display some unusual properties in the presence of magnetic fields. Despite extensive research[1] during the last three years, most of which has focused on dissipative effects at high fields, important parameters which define the mixed state, such as the lower critical field H_{c1} and pinning force constants, are still poorly determined. In this work, we present direct measurements of these parameters, via sensitive measurements of the field-dependent penetration depth in $YBa_2Cu_3O_y$ crystals.

The penetration depth is a probe of the condensate fraction of order parameter, and is particularly sensitive to changes induced by external magnetic fields. In the Meissner state, the external field causes homogeneous changes of the order parameter, while it induces spatially inhomogeneous excitations (i.e., vortices) in the mixed state. These effects are probed in the present experiment by radio-frequency (6 MHz) currents induced by small rf fields $\mathbf{H}_\omega$ applied perpendicularly to the $\hat{\mathbf{c}}$ axis. The sample is placed in a small 20-turn tightly wound coil, which forms part of the tank circuit of an ultrastable tunnel diode oscillator. Changes $\Delta\lambda$ in the penetration depth due to a static magnetic field $\mathbf{H}$ are measured as resonant frequency shifts $\Delta f(H)$, by $\Delta\lambda(H)\equiv\lambda(H)-\lambda(0)=-G\Delta f(H)$, where G (typically ~10 Å/Hz) is a geometric factor. The very high stability of the oscillator (1 Hz in 6×10^6 Hz) enables a resolution of ~10 Å, which is essential to observe the effects reported here. In all the experiments discussed here, $\mathbf{H}_\omega\perp\hat{\mathbf{c}}$ always, while $\mathbf{H}$ is oriented perpendicularly or parallel to $\hat{\mathbf{c}}$. The rf response is determined by the dc flux density in the sample (as we show below), and the data directly yield $H_{c1}(T)$, the functional dependence $B(H)$, and the pinning force constant $\alpha(T)$, in both orientations and over the entire temperature range 4.2 K to T_c.

High-quality $YBa_2Cu_3O_y$ crystals were fabricated as discussed in Ref. 2. Detailed measurements of several electrodynamic parameters, viz., $\lambda_{ab}(T)$, $R_s(T)$, the pair-breaking parameter $k(T)$, and also the lower critical-field $H_{c1\perp}(T)$, have been reported earlier,[3] and are found to obey temperature dependences in good agreement with BCS calculations. Thus these crystals, which have extremely sharp transitions, are well characterized as regards their electrodynamic properties in the Meissner state.

Typical results for $\Delta\lambda$ vs $\mathbf{H}$ ($\parallel\hat{\mathbf{c}}$) are shown in Fig. 1 at $T=9.7$ K. $\Delta\lambda=0$ in the Meissner state, until the critical field $H^0_{c1\parallel}$ is reached signaling the entry of flux. Here $H^0_{c1\parallel}=H_{c1\parallel}/\mathfrak{N}$ is the bulk critical field reduced by the demagnetization factor $\mathfrak{N}$. For $H>H^0_{c1\parallel}$, $\Delta\lambda$ increases with a field dependence which is *sublinear*.

In Fig. 1 *the break at $H^0_{c1\parallel}$ is sharp and unambiguous.* In general, the rf measurements appear to yield much cleaner signatures for H_{c1} compared to magnetization data—we believe this to be due to the very high sensitivity of the rf technique. The resolution limit of $\Delta\lambda=10$ Å corresponds to $\Delta M/M\sim2\times10^{-5}$ for a sample 50 μm thick, when $\mathbf{H}\perp\hat{\mathbf{c}}$.

Combining the parallel and perpendicular measurements (the latter are shown in Fig. 2), the temperature dependence of H_{c1} both parallel and perpendicular to $\hat{\mathbf{c}}$,

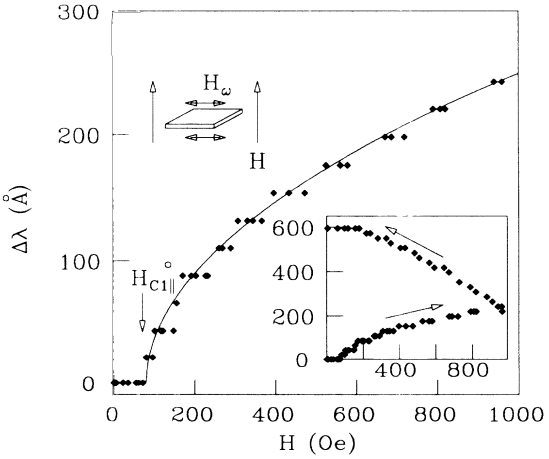

FIG. 1. $\Delta\lambda(H)\equiv\lambda(H)-\lambda(0)$ vs $\mathbf{H}$ ($\parallel\hat{\mathbf{c}}$) at $T=9.7$ K. Note the sharp break at $H^0_{c1\parallel}$, and the sublinear dependence for large fields (the line is a guide to the eye). Top inset: Field configuration. Bottom inset: Complete behavior for field cycling.

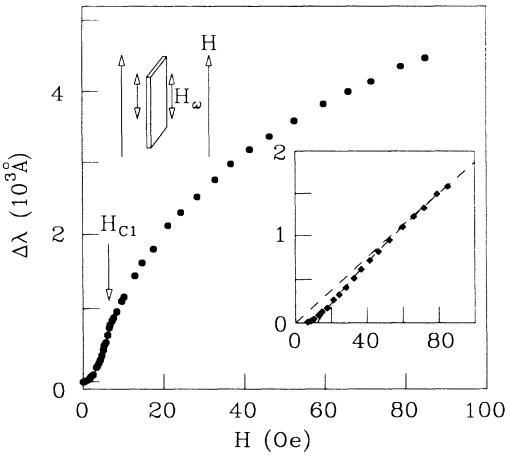

FIG. 2. $\Delta\lambda(H)$ vs $\mathbf{H}$ ($\perp\hat{\mathbf{c}}$) at $T=84.5$ K. Top inset: Field configuration. Bottom inset: $[\Delta\lambda(H)-\Delta\lambda(H_{c1})]^2$ (10^7 Å) vs $\mathbf{H}$.

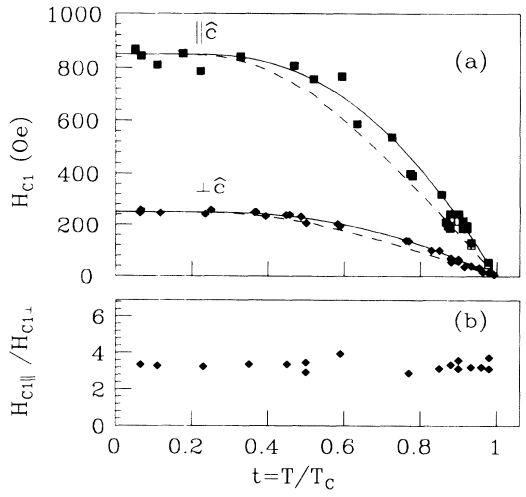

FIG. 3. (a) Temperature dependence of H_{c1} in both the $\|\hat{\mathbf{c}}$ and $\perp\hat{\mathbf{c}}$ configurations. The lines represent BCS calculations, with gap ratios $2\Delta/kT_c=4.3$ (solid) and 3.5 (dashed). (b) Temperature dependence of the anisotropy ratio $H_{c1\|}/H_{c1\perp}$.

measured for the *same sample* ($T_c=88.2$ K), is displayed in Fig. 3. For $\mathbf{H}\|\hat{\mathbf{c}}$, $H_{c1\|}=\Re H^0_{c1\|}$ with $\Re=11$ (and temperature independent) for this sample, estimated assuming an ellipsoidal shape (dimensions 1×1 mm$^2\times50$ μm). The $\mathbf{H}\perp\hat{\mathbf{c}}$ data (here $H_{c1\perp}=H^0_{c1\perp}$) are identical to those reported[3] earlier using the same technique on another sample. (As shown in Fig. 2 of Ref. 3, the H_{c1} signature in this configuration is also sharp and unambiguous.) The demagnetization effects were carefully checked with calibrations using Nb platelets of approximately the same dimensions as the $YBa_2Cu_3O_y$ samples. These calibration measurements confirm the demagnetization calculations and the magnitudes reported here.

The *BCS-like character of H_{c1} in both configurations* is evident. We find $H_{c1\|}(0)=850\pm40$ Oe, and $H_{c1\perp}(0)=250\pm20$ Oe. These values lead to an anisotropy of 3.4 ± 0.3, which within the uncertainty in the measurement, appears to be temperature independent [Fig. 3(b)]. The H_{c1} anisotropy may be compared with other results,[4] which typically range from 2.9 to 5.8.

For an *anisotropic superconductor,*[5] in the present notation, $H_{c1\|,\perp}=[\phi_0/4\pi\lambda_\|\lambda_{\|,\perp}][\ln(\sqrt{\lambda_\|\lambda_{\|,\perp}}/\xi_\|\xi_{\|,\perp})+0.5]$. Ignoring the logarithmic term, the field anisotropy can be used to deduce a mass anisotropy of

$$m_\|/m_\perp\propto\lambda_\|^2/\lambda_\perp^2\propto(H_{c1\|}/H_{c1\perp})^2=11.6$$

at 4.2 K. It appears that torque magnetometry[6] and magnetic anisotropy[7] measurements tend to yield higher values ~25 to 64, while as noted above, H_{c1} measurements tend to give lower values. To our knowledge the present work is the first complete and direct determination of the anisotropy temperature dependence. The mean-field behavior of H_{c1} and the absence of any temperature dependence in the anisotropy validates the use of anisotropic Ginzburg-Landau theory.

The temperature dependence of H_{c1} in both directions is in good agreement with BCS calculations, as shown in Fig. 3 as the solid lines. Here we have used $H_{c1}\propto1/\lambda^2(T)$, and employed detailed numerical BCS calculations[3] with a variable gap parameter $2\Delta/kT_c$. As Fig. 3 shows, best fits are obtained for $2\Delta/kT_c=4.3$, with less satisfying fits for 3.5, in agreement with our earlier findings[3] on the temperature dependence of electrodynamic properties.

We now turn to understanding the features of the $\Delta\lambda(H)$ data in Figs. 1 and 2. In the Meissner state ($H<H^0_{c1}$), $\Delta\lambda(H)=0$ for $\mathbf{H}\|\hat{\mathbf{c}}$, and $\Delta\lambda(H)=k(T)H^2$ for $\mathbf{H}\perp\hat{\mathbf{c}}$. The quadratic dependence in the latter case is well understood to be due to pair breaking by the applied static field, and the temperature dependence of $k(T)$ is very well described[3] by a Ginzburg-Landau model. This is not observed when $\mathbf{H}\|\hat{\mathbf{c}}$ and $\mathbf{H}_\omega\perp\hat{\mathbf{c}}$ because the dc and rf currents only superpose over a periphery of width λ of the sample, and hence the pair-breaking quadratic dependence (determined by an overlap integral $\int H^2H_\omega dS$ over the sample area S) is very small and unobservable.

We next turn to the data for $H>H^0_{c1\|}$ when $\mathbf{H}\|\hat{\mathbf{c}}$. In the mixed state, the rf induced current of density J_ω creates an oscillating Lorentz force which acts on the vortices, causing them to oscillate about their equilibrium positions. Start from the equation of motion for the displacement x_ω: $\eta\dot{x}_\omega+\alpha x_\omega=f_L=\phi_0J_\omega$, where η and α are the damping coefficient and the pinning force constant, respectively. From the electric field $E_\omega=B\dot{x}_\omega$, it is easy to show that the oscillatory vortex response leads to a constitutive relation $J_\omega=[(\alpha-i\omega\eta)/(-i\omega\phi_0B)]E_\omega$, from which we obtain for the penetration depth

$$\lambda^2(H,T)=[\phi_0/\mu_0\alpha(T)]B(H)\,. \qquad (1)$$

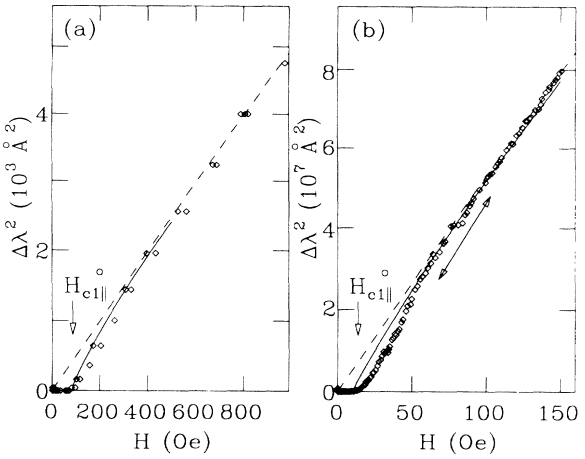

FIG. 4. $\Delta\lambda^2(H)$ vs $\mathbf{H}$ ($\|\hat{\mathbf{c}}$) for (a) 9.7 K and (b) 84 K (including field-reversed data). Note that the $H \gg H_{c1\|}^0$ behavior linearly extrapolates through the origin. The solid lines represent calculations based on Ref. 10.

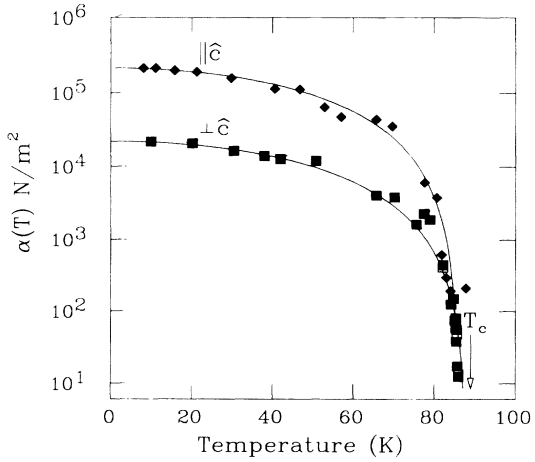

FIG. 5. Temperature dependence of the pinning force constant $\alpha(T)$. The lines represent a $[1-(T/T_c')^2]^2$ dependence.

Equation (1) shows that the rf $\lambda(H)$ measurements can be interpreted to yield, first, the dc magnetic flux density $B(H)$ inside the sample, and also the pinning parameter $\alpha(T)$. In Figs. 4(a) and 4(b), we plot $\Delta\lambda^2(H)$ vs H for two temperatures, 9.7 and 85 K. The functional dependence is remarkably similar to the classic[8] $B(H)$ dependence expected for type-II superconductors. For $H \gg H_{c1\|}^0$, the data clearly coincide with a linear H dependence[9] at all temperatures [Figs. 4(a) and 4(b)] passing through the origin, as $B(H)$ should. We have attempted to compare the data with detailed predictions for $B(H)$ at lower fields near H_{c1}. In Figs. 4(a) and 4(b), the solid lines represent Nelson's[10] form $B(H) \propto (H-H_{c1\|}^0)\ln[H'/(H-H_{c1\|}^0)]$, which is in reasonable agreement at low temperatures. For $H \gtrsim H_{c1\|}^0$ the data show an increasing rounding with increasing temperature at the onset of flux entry. Thus a functional form $B(H) \propto (H-H_{c1\|}^0)^{\beta(T)}$ appears to best describe the data in the intermediate-field range $H_{c1}^0 < H < 4H_{c1}^0$, with $\beta = 1$ at low temperatures [Fig. 4(a)] and $\beta > 1$ with increasing temperature [$\beta \approx 1.5$ at 85 K in Fig. 4(b)]. This is consistent with some calculations[10,11] of $B(H)$ near H_{c1}, and the temperature dependence suggests that line wandering increases with increasing temperature.

In the configuration $\mathbf{H} \perp \hat{\mathbf{c}}$, the behavior of $\Delta\lambda$ vs H is qualitatively similar for $H > H_{c1\perp}$, in that a sublinear field dependence is also observed. Here the driving force arises from the flux density gradient dB/dx, and an analysis similar to that of Campbell and Evetts[12] again yields Eq. (1). This is confirmed experimentally in the plot of $[\Delta\lambda(H)-\Delta\lambda(H_{c1})]^2$ vs H shown in the inset to Fig. 2. Again at high fields a linear behavior is observed, extrapolating to the origin. [The condensate effects appear to be adequately accounted for by the subtraction of the pair-breaking contribution evaluated at H_{c1}, i.e., $\Delta\lambda(H_{c1})$. It should be noted that this does not affect the high-field behavior, which is discussed next.]

From the data shown in Figs. 2 and 4, we extract a high-field ($H \gtrsim 4H_{c1}^0$) limiting slope, and from it obtain the pinning force constants $\alpha_\|$ and $\alpha_\perp$ in both directions. The temperature dependence of α is shown in Fig. 5. The pinning force depends on field orientation, with $\alpha_\|(0) = 2.2\times10^5$ N/m^2 and $\alpha_\perp(0) = 2.1\times10^4$ N/m^2. Elementary vortex-core-pinning considerations suggest that $\alpha \approx B_c^2/2\mu_0$. This yields $B_{c\|}(0) = 0.8$ T and $B_{c\perp}(0) = 0.25$ T. These values are in excellent agreement with other estimates.[13] The relation between α and B_c also suggests a $(1-t^2)^2$ dependence. Indeed this is exactly what the data seem to obey, as shown by the solid lines representing $[1-(T/T_c')^2]^2$ in Fig. 5. Interestingly, $T_c' = 87$ K ($\mathbf{H} \perp \hat{\mathbf{c}}$) and ~ 86.2 K ($\mathbf{H} \| \hat{\mathbf{c}}$), both below the bulk $T_c = 88.2$ K, which is defined as the (sharp) peak in the temperature derivative $[d\Delta\lambda(T)/dT]$ of the $\lambda(T, H=0)$ data. This implies that the pinning forces vanish slightly below the mean-field transition temperature. Between T_c' and T_c, the exact behavior is not clear, with $\alpha_\|$ appearing to increase again. A detailed study of this region is the subject of future work.

A comparison with results on polycrystals is interesting. The data are similar to the $\mathbf{H} \perp \hat{\mathbf{c}}$ results of Fig. 2; however, the field dependence is enormous. We obtain $\alpha(0) = 4.2$ N/m^2, which is 10^3–10^4 smaller than for the single crystals. This is understandable because of the extremely weak pinning of the intergranular vortices.[14,15]

We next explore the relationship of our experiments to others on high-T_c superconductors. Note that our measurements are *reactive* (nondissipative), and measure the in-phase ac response at the fundamental driving frequency. This necessarily requires a flux response proportional to displacement, i.e., a restoring force $-\alpha x$. Since $H_\omega \sim 10$ mOe, the probe current $J_\omega \sim 10^{-3}$ A/cm^2, which is much lower than in resistivity measurements. The vortices are taken to execute reversible oscillations, which are of amplitude $\ll 1$ Å. We have tested and

found the results to be independent of the ac field over a small range of the rf field (the tunnel-diode-oscillator circuit allows current variations only by a factor of 2). The analysis is based on the reasonable assumption that α is field independent, at least at the low fields studied here. A very high fields, α may be expected to decrease —indeed high-field studies, which is the subject of future work, might be expected to distinguish between various theories of flux behavior (e.g., flux lattice melting, flux creep, vortex glass, etc.).

The interplay between elastic and viscous forces determines the crossover frequency $f_0=\alpha/\eta=\alpha\rho_n/\phi_0 B_{c2}$, where ρ_n ($\approx 50\ \mu\Omega$ cm) is the normal-state resistivity, and B_{c2} is the upper critical field. Assuming[16] $B_{c2}=26$ T at 77 K, we get $f_0\sim 9.6\times 10^{10}$ Hz at 77 K. This may be compared to $\sim 10^8$ Hz for low-T_c superconductors.[17]

It is possible to estimate a single-vortex depinning critical current if one assumes, for example, a sinusoidal potential well $U(x)=(-U_0/2)\cos(\pi x/L)$, where L is the well dimension. Our measurements yield the curvature at low x through the relation $\alpha=\pi^2 U_0/2L^3$. Equating the maximum pinning force to a maximum Lorentz force, one gets $J_{c0}=L\alpha/\pi\phi_0$. Using[16] $L\sim 70$ Å, we get $J_{c0\parallel}\sim 2.5\times 10^7$ A/cm^2 and $J_{c0\perp}\sim 2.3\times 10^6$ A/cm^2, from the measured values of α at low temperatures. These values should be regarded as upper limits to achievable critical currents in single crystals. (The polycrystalline data naturally imply much smaller values, $J_{c0}\sim 10^3$ A/cm^2). Furthermore, the observed magnitude of α is consistent with a barrier height of $U_0\sim 10^3$ K and a well volume of $L^3\sim 3.5\times 10^5$ Å^3, which may be compared with the observed thermal activation energies in critical-current experiments.[16,18] From $\alpha\sim F_p L$, we deduce pinning force densities of 3.1×10^{13} N/m^3 ($\parallel\hat{c}$) and 3.0×10^{12} N/m^3 ($\perp\hat{c}$), which appear to be larger than those calculated by Kes and van den Berg[19] for pinning by twin boundaries. Our interpretation of the data is consistent with densely populated pinning centers,[20] and pinning due to twin boundaries is not unlikely to be the dominant cause in our crystals.[21]

Our results are significant for several reasons. First, they provide the *complete* low-field H-T phase diagram in $YBa_2Cu_3O_y$ crystals, particularly the H_{c1} phase boundary and its anisotropy. Further, the $\lambda(H)$ measurements are a probe of the constitutive relations governing the superconductor. In the Meissner state, the $\lambda(H)$ data test the nonlinear London relation $J=-Q_1A-Q_2A$,[3] wherein pair-breaking effects manifest themselves as $\Delta\lambda=kH^2$, and are measured via the pair-breaking parameter k ($\equiv d\Delta\lambda/dH^2$) which is $\propto Q_2$. In the mixed state, the $\lambda(H)$ data yield the $B(H)$ constitutive relation for the first time, and the derivative $\alpha\propto(d\Delta\lambda^2/dH)^{-1}$ is a measure of the pinning forces. The pinning parameter α (also known as the Labusch parameter) determined in this work is an important parameter which enters into the analysis of other experiments, and in theories of the flux state. In contrast to dissipative (e.g., resistivity) measurements, the *reactive* measurements carried out here probe the thermodynamic, quasiequilibrium properties of the superconductor in the presence of a magnetic field.

This work was supported by NSF-ECS-8811254 and by the U.S. Air Force Systems Command, Rome Air Development Center. We thank J. R. Clem and R. S. Markiewicz for useful discussions.

[1] *Physical Properties of High T_c Superconductors,* edited by D. M. Ginzberg (World Scientific, Singapore, 1989).

[2] Dong Ho Wu, W. Kennedy, C. Zahopoulos, and S. Sridhar, Appl. Phys. Lett. **56**, 696 (1989).

[3] S. Sridhar, Dong-Ho Wu, and W. Kennedy, Phys. Rev. Lett. **63**, 1873 (1989).

[4] L. Krusin-Elbaum *et al.*, Phys. Rev. B **39**, 2936 (1989); A. Umezawa *et al.*, Phys. Rev. B **38**, 2843 (1988).

[5] R. A. Klemm and J. R. Clem, Phys. Rev. B **21**, 1868 (1980).

[6] D. Farrel *et al.*, Phys. Rev. Lett. **64**, 1573 (1990); **61**, 2805 (1988).

[7] M. Tuominen, A. M. Goldman, Y. Z. Chiang, and P. Z. Jiang, Phys. Rev. B **42**, 412 (1990).

[8] M. Tinkham, *Introduction to Superconductivity* (McGraw-Hill, New York, 1979).

[9] A. F. Hebard, P. L. Gammel, C. E. Rice, and A. F. J. Levi, Phys. Rev. B **40**, 5243 (1989). In this work, a $\sqrt{H}$ dependence of $\lambda(H)$ has been observed in mutual-inductance measurements on thin films at high fields. The reported magnitudes of $d\lambda/d\sqrt{H}$ are in excellent agreement with our data for $\mathbf{H}\parallel\hat{c}$.

[10] D. R. Nelson, Phys. Rev. Lett. **60**, 1973 (1988).

[11] T. Natterman and R. Lipowsky, Phys. Rev. Lett. **61**, 2508 (1988).

[12] A. M. Campbell and J. Evetts, Adv. Phys. **21**, 199 (1972).

[13] M. B. Salomon and J. Bardeen, Phys. Rev. Lett. **59**, 2615 (1987).

[14] J. Clem, in *Proceedings of the International Conference on Superconductivity, Stanford, CA, 1989* [Physica (Amsterdam) **162-164**, 1137 (1989)].

[15] J. Halbritter, J. Appl. Phys. (to be published).

[16] A. P. Malozemoff *et al.*, in *Strong Correlations and Superconductivity,* edited by H. Fukuyama *et al.* (Springer-Verlag, Heidelberg, 1989).

[17] J. Gittleman and B. Rosenblum, Phys. Rev. Lett. **16**, 734 (1966).

[18] T. T. M. Palstra, B. Batlogg, R. B. van Dover, L. F. Schneemeyer, and J. V. Waszczak, Appl. Phys. Lett. **54**, 763 (1989).

[19] P. Kes and J. van den Berg, in "Studies of High Temperature Superconductors," edited by A. V. Narlikar (Nova Science, New York, to be published).

[20] M. Inui, P. B. Littlewood, and S. N. Coppersmith, Phys. Rev. Lett. **63**, 2421 (1989).

[21] Good quality samples such as those studied here generally show a low twin density.